



## INTERNATIONAL JOURNAL OF PURE AND APPLIED RESEARCH IN ENGINEERING AND TECHNOLOGY

A PATH FOR HORIZING YOUR INNOVATIVE WORK

### XRD AND FTIR STUDIES OF ARGON ION IMPLANTATION INTO MANGANESE DEPOSITED GALLIUM ANTIMONIDE THIN FILMS

N. S. PRADHAN<sup>1</sup>, S. K. DUBEY<sup>2</sup>

1. Department of Physics, Ramnarain Ruia College, Mumbai, India.
2. Department of Physics, University of Mumbai, Mumbai, India.

Accepted Date: 27/02/2014 ; Published Date: 01/05/2014

**Abstract:** The effect of implantation of 250 keV Argon ions in manganese deposited p- type GaSb at  $5 \times 10^{15}$  to  $1 \times 10^{16}$  ions  $\text{cm}^{-2}$  were investigated by Fourier Transform Infra Red Spectrometer [FTIR], X-ray Diffraction techniques. XRD techniques have been used to investigate the bombardment effects. FTIR transmission studies showed that the optical density of manganese deposited GaSb implanted with different fluence increases near the band edge with increase in the ion fluence. The density of defect in the samples implanted with different ion fluences was in the range of  $1.2 \times 10^{14}$ -  $20.7 \times 10^{15}$   $\text{cm}^{-3}$ . The tailing energy estimated from the transmission spectra was found to change from 4.0 to 8.8 meV with increase in ion fluence.

**Keywords:** GaSb; Argon Ion; XRD; FTIR.

Corresponding Author: MR. N. S. PRADHAN



PAPER-QR CODE

Access Online On:

[www.ijpret.com](http://www.ijpret.com)

How to Cite This Article:

NS Pradhan, IJPRET, 2014; Volume 2 (9): 118-126

## INTRODUCTION

Gallium antimonide is a narrow band gap III-V compound semiconductor has received increasing importance because of its potential applications in optoelectronics devices such as long wavelength photo-detector and light emitting diodes. Some studies on the effects of ion implantation in III-V compound semiconductors, including GaSb, with different ions like Si, Mg, S, Se, Ne, and Ar have been reported. The characteristics of Si and Mg ions in InAs, GaSb and GaP with fluences varying from  $5 \times 10^{15}$  to  $1 \times 10^{16}$  ions  $\text{cm}^{-2}$  at 100 eV investigating using transmission electron microscope (TEM). Rutherford backscattering spectroscopy (RSB) and secondary mass spectroscopy showed the amorphization of the surface [1]. The annealing of structure defects caused by implanting the silicon in GaSb with fluence from  $1 \times 10^{13}$  to  $1 \times 10^{15}$  ions  $\text{cm}^{-2}$  at different energies (70-150 keV) have been studied by Raman spectroscopy[2]. The recovery of damaged layer was found to be better after rapid thermal annealing at  $600^\circ\text{C}$  for 30s. Amorphization of elemental and compound semiconductors by implanting silicon ion with fluence from  $1 \times 10^{14}$  to  $1 \times 10^{16}$  ions  $\text{cm}^{-2}$  at 20 keV has been investigated by cross sectional TEM [3]. The production and annealing of radiation damage in GaSb by 1.8 MeV  $\text{Ne}^+$  implanted with fluences of  $5 \times 10^{13}$ ,  $2.5 \times 10^{14}$  and  $1 \times 10^{15}$  ions  $\text{cm}^{-2}$  were studied by TEM and RSB in combination with channeling technique [4]. GaSb and InSb can be rendered porous with ion irradiation under the appropriate implant conditions. Although several theories have been proposed, the operative mechanism is still under investigation [5]. The continuous to porous transformation has been compared with the ion induced porosity observed in Ge [6]. However, in Ge porosity is only observed for doses significantly greater than the amorphization threshold. In the antimonides, on the other hand, both the crystalline to amorphous and continuous to porous transformations occur at similar doses. Previous investigations have concentrated on porosity [7]. The porosity induced by Ga ion irradiation have been investigated as a function of ion implant doses [8]. In an earlier work, we have presented the detailed results of the structural and optical studies of n- GaSb crystals bombarded with different fluences of argon ions at 250 keV [9]. In the present work, we have reported structural and optical properties using Fourier Transform Infra Red Spectrometer (FTIR) and single crystal X-ray diffractometer (XRD) techniques.

## I. EXPERIMENTAL DETAILS

The single crystal p-GaSb samples mirror polished <100> orientation and thickness  $\sim 500 \mu\text{m}$  were cleaned using the electronic grade organic solvents. The high purity manganese metal thin film approximately 25 nm thick were deposited on clean gallium arsenide substrate in vacuum of  $10^{-6}$  Torr. The filament current was maintained between 30- 40 ampers during deposition.

These deposited samples were implanted with argon ions for various ion fluences varying from  $5 \times 10^{15}$  to  $5 \times 10^{16}$  ions  $\text{cm}^{-2}$  at 250 keV. The beam was scanned over  $2.5 \text{ cm} \times 2.5 \text{ cm}$  area on sample surface for uniform implantation. The beam current was about 2 to 3  $\mu\text{A}$  during the implantation at  $10^{-6}$  mbar. X-ray diffractometer XRD profiles of the samples were recorded on Panalytical Xpert [PRO,Cu anode, 40kV/30mA] RTMS detector. FTIR transmission spectra for non-implanted, manganese deposited and implanted gallium antimonide samples were recorded in the spectral region  $6000$  to  $400 \text{ cm}^{-1}$  using the Fourier Transform Infra Red Spectrometer.

## II. RESULTS AND CONCLUSION

### A. X-ray Diffraction (XRD) Studies

Figure 1(a)-1(d) shows the XRD spectra of non-implanted and 250 keV argon ions implanted into manganese deposited gallium antimonide for the fluencies of  $5 \times 10^{15}$ ,  $1 \times 10^{16}$  and  $5 \times 10^{16}$  ions  $\text{cm}^{-2}$  respectively. XRD study of gallium antimonide sample showed peaks at  $29.24^\circ$  and  $60.57^\circ$  attributed from (002) and (004) reflections respectively. The peak intensity and full width at half maximum (FWHM) for  $\langle 400 \rangle$  reflection obtained with  $K_{\alpha 1}$  and  $K_{\alpha 2}$  has been obtained from the spectra is compared in the Figure 1. It has been observed that the XRD peak intensity of implanted samples decreases with ion fluence. The values of full width at half maximum were found to be decreased for  $5 \times 10^{15}$  ions  $\text{cm}^{-2}$ , whereas increased for the sample implanted with  $5 \times 10^{16}$  ions  $\text{cm}^{-2}$ . These change in peak intensity and FWHM indicates the amount of disorder and defect concentration in the samples. The shift of the XRD peak with ion fluence indicates the presence of strain and change in the lattice parameter [9]. The strain present in the implanted samples has been estimated from the peak shift using the relation;

$$\varepsilon = \frac{d_n - d_0}{d_0} \quad (1)$$

where  $d_n$  and  $d_0$  are the inter planar spacing of the implanted and non-implanted samples respectively.

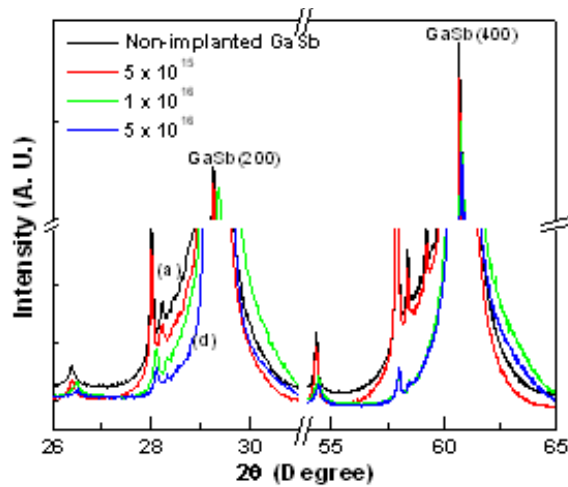


**Figure 1:** X-ray diffraction spectra of (a) non- implanted and 250 keV Ar<sup>++</sup> implanted into manganese metal deposited gallium antimonide for the fluences of; (b)  $5 \times 10^{15}$ , (c)  $1 \times 10^{16}$ , (d)  $5 \times 10^{16}$  ions  $\text{cm}^{-2}$ .

**TABLE-I:** Strain and crystalline size in the Mn deposited GaSb samples implanted with 250 keV Ar<sup>++</sup> ion estimated from XRD reflection.

Ion fluence (ions $\text{cm}^{-2}$ )	Strain	Crystalline size (nm)
$5 \times 10^{15}$	$1.7 \times 10^{-4}$	123
$1 \times 10^{16}$	$3.3 \times 10^{-3}$	97
$5 \times 10^{16}$	$3.7 \times 10^{-3}$	103

Ion implantation induced strain in the implanted samples were found to vary as shown in table-I. It has observed that the size of crystallite changes with fluence, calculated from figure 1. Full width of half maximum

using the following relation [9].

$$FWHM = \frac{0.9\lambda}{t \cos \theta} \quad (2)$$

where t is the size of crystallite,  $\lambda$  (1.5405 A.U.) is the wavelength of Cu-K<sub>α1</sub> radiation and  $\theta$  is the Bragg's angle. The crystalline size and strain found to vary with ion fluences as shown in TABLE-I.

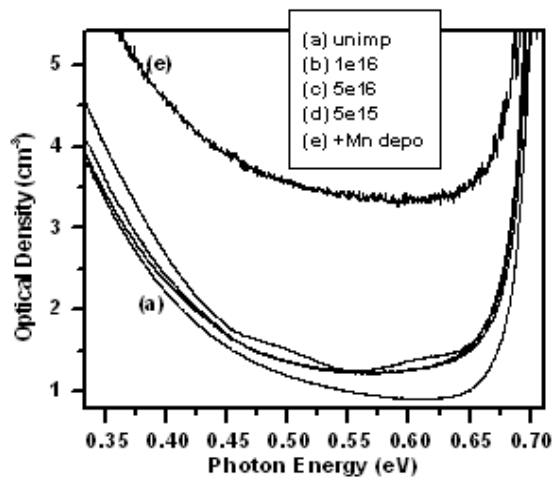
### B. Fourier Transform Infra Red (FTIR) Studies

Figure 2(a)-2(e) shows the FTIR transmission spectra of non implanted, Mn deposited and 250 keV argon ions implanted into Mn deposited gallium antimonide with various fluences ranging from  $5 \times 10^{15}$  to  $5 \times 10^{16}$  ions  $\text{cm}^{-2}$  samples respectively. It can be observed from Figure that the transmission intensity decreased with increasing ion fluence. The decrease in the intensity is due to radiation induced defects.

To estimate the defect densities in the implanted samples and Manganese deposited sample. The absorption coefficient ( $\alpha$ ) has been determined using the following equation, taking into account the multiple reflections [10]:

$$\frac{I}{I_0} = \frac{(1-R)^2 e^{-\alpha d}}{1-R^2 e^{-2\alpha d}} \quad (3)$$

Where  $I_0$ ,  $I$  are the incident and transmission intensities respectively,  $d$  ( $\sim 500 \mu\text{m}$ ) is the thickness of the sample and  $R$  is the reflectivity and determined from the refractive index of gallium antimonide .



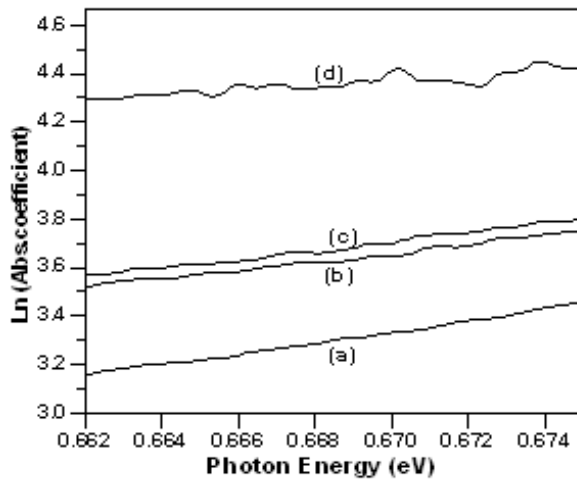
**Figure 2:** Optical density ( $\alpha.d$ ) verses photon energy ( $h\nu$ ) curves; (a) non implanted GaSb and 250 keV  $\text{Ar}^{++}$  ion implanted into Mn deposited GaSb with difference fluences of; (b)  $5 \times 10^{15}$ , (c)  $1 \times 10^{16}$ , (d)  $5 \times 10^{16} \text{ cm}^{-2}$ , (e) Mn deposited GaSb.

It is seen that the optical density ( $\alpha.d$ ) of sample implanted with  $5 \times 10^{15}$  ions  $\text{cm}^{-2}$  near band gap edges indicates the increase in the defect concentration compare with the non-implanted sample [Fig.2(d)]. This shows the considerable decrease in the defect concentration above mid

gap region. To understand the crystalline nature of the implanted gallium antimonide samples, the following Urbach relation [11] has been used in the lower energy range to compute the tailing energy;

$$\alpha = \alpha_0 \exp\left(\frac{h\nu}{E_0}\right) \quad (4)$$

Where,  $E_0$  is the band tail energy.



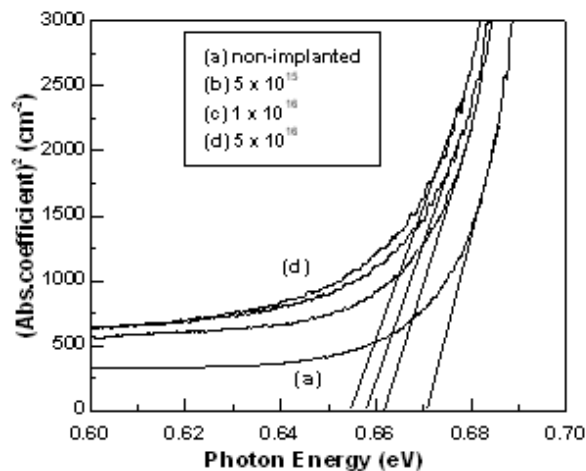
**Figure 3:**  $\ln(\alpha)$  versus photon energy( $h\nu$ ) plots of; (a) non implanted GaSb and 250 keV  $\text{Ar}^{++}$  ion implanted into Mn deposited GaSb with the difference fluence of; (b)  $5 \times 10^{15}$  ion  $\text{cm}^{-2}$ , (c)  $1 \times 10^{16}$  ions  $\text{cm}^{-2}$ , (d)  $5 \times 10^{16}$  ions  $\text{cm}^{-2}$ .

Figure 3(a)-(d) shows the  $\ln\alpha$  versus photon energy curves of non implanted and 250 keV argon implanted into Mn deposited gallium antimonide with various fluence ranging from  $1 \times 10^{15}$  to  $5 \times 10^{16}$  ions  $\text{cm}^{-2}$  respectively. The calculated values of band tail ( $E_0$ ) in the fundamental edge found be to increased from 4 meV to 9 meV as the fluence increased from  $5 \times 10^{15}$  to  $5 \times 10^{16}$  ions  $\text{cm}^{-2}$  at 250 keV and observed 60 meV for manganese deposited gallium antimonide sample. Whereas the corresponding estimate for the non-implanted gallium antimonide found to 4 meV. The increase of band tails indicates the decrease of crystallinity at higher fluence.

The defect densities of implanted samples were estimated from **Figure 2**, using the following relation [12].

$$N_s = \mu \left[ \frac{m_e c}{2\pi^2 e^2 \hbar} \right] \left[ \frac{3}{\mu^2 + 2} \right]^2 \frac{1}{f} \int \alpha(\text{excess}) dE. \quad (5)$$

Where,  $\int \alpha(\text{excess}) dE$  is the difference in the areas of non- implanted samples extracted from figure 1,  $\mu$  the refractive index,  $c$  the speed of light,  $e$  the electron charge and  $f$  the oscillator strength and has been assume to be one. In this calculation, it is assumed that total area of the optical density ( $\alpha.d$ ) versus photon energy plot presented the total density of radiation induced defect states. The density defects in the sample implanted with  $5 \times 10^{15}$ ,  $1 \times 10^{16}$  and  $5 \times 10^{16}$  ions  $\text{cm}^{-2}$  were found to be  $1.2 \times 10^{14}$ ,  $1.88 \times 10^{15}$  and  $20.7 \times 10^{15} \text{ cm}^{-3}$  respectively. To estimate the band gap energy,  $\alpha^2$  versus  $h\nu$  graph for non implanted and implanted samples with different fluences has been plotted shown in Figure 4. The straight line portion extrapolated at  $\alpha^2 = 0$  gives the band gap energy [13]. The value of band gap energy for argon ions implanted into Mn deposited GaSb samples with fluences  $5 \times 10^{15}$ ,  $1 \times 10^{16}$  and  $5 \times 10^{16}$  ions  $\text{cm}^{-2}$  were found to be 0.664, 0.658 and 0.654 eV respectively. Whereas the corresponding estimate for the non-implanted sample was 0.672 eV. The changes in the band gap energy due to amorphization of the GaSb surface.



**Figure 4:**  $\alpha^2$  versus photon energy ( $h\nu$ ) plots of; (a) non implanted GaSb and 250 keV  $\text{Ar}^+$  ion implanted with difference fluences of; (b)  $5 \times 10^{15}$ , (c)  $1 \times 10^{16}$ , (d)  $5 \times 10^{16} \text{ cm}^{-2}$ .

### III. CONCLUSION

The non-implanted, manganese deposited and 250 keV  $\text{Ar}^+$  ions implanted into Mn deposited GaSb with various fluences has been studied using XRD and FTIR techniques. FTIR studies reveal the increase of defect density with ion fluence. The material losses crystallinity and leads

towards amorphization as indicated by the increase in tailing energy of implanted samples. XRD theory showed the size of crystallite changes with ion fluences, also indicates the presence of strain and change in the lattice parameter.

## REFERENCES

1. S. J. Pearton, A. R. Von Neida, J. M. Brown et al., J. Appl. Phys. 64 (2) 629 (1988).
2. Y. K. Su, K. J. Gan, J.S.Hwang et. Al, J. Appl. Phys. 68 (11) 5584 (1990).
3. K. S. Jones and C. J. Santana, J. Mater. Res. 6(5) 1048 (1996).
4. R. Callec and A. Poudoulec, J. Appl. Phys. 73 (10) 4831 (1993).
5. N. Nitta, M. Taniwaki, Y. Hayashi and T. Yoshiie, App. phys. 92, 1799 (2002).
6. L. Wang and R. Birtcher, Philos, Mag. A. 64, 1209 (1991).
7. R. Callec and A. Poudoulec, J.Appl.Phys. 73, 4831 (1993).
8. Kluth, Fitz Gerald, and Ridgway, J.Appl.Phys letters 86,131920 (2005).
9. S. K. Dubey, S. D. Pandey, R. L. Dubey, A. D. Yadav, Radiat. Eff. and defect in solid, 161, 7, 433-442 (2006).
10. J. R. Ferraro and K. Krishnan, Practical Fourier Transform Infrared Spectroscopy Academic Press Inc., San Diego (1990).
11. S. Nooh, A. Bakry, H. El-Zahed et al., Radiat. Eff. Defects Solids 159 561 (2004).
12. D. L. Dexter, Phys. Rev. B 101 48 (1956).
13. J. I. Pankove, Optical Processes in Semiconductors, Prentice-Hall, Englewood Cliffs, (1971).